



Regulation of Replication Fork Progression Through Histone Supply and Demand

Anja Groth, *et al.*

Science **318**, 1928 (2007);

DOI: 10.1126/science.1148992

The following resources related to this article are available online at www.sciencemag.org (this information is current as of January 3, 2008):

Updated information and services, including high-resolution figures, can be found in the online version of this article at:

<http://www.sciencemag.org/cgi/content/full/318/5858/1928>

Supporting Online Material can be found at:

<http://www.sciencemag.org/cgi/content/full/318/5858/1928/DC1>

This article **cites 25 articles**, 11 of which can be accessed for free:

<http://www.sciencemag.org/cgi/content/full/318/5858/1928#otherarticles>

This article appears in the following **subject collections**:

Molecular Biology

http://www.sciencemag.org/cgi/collection/molec_biol

Information about obtaining **reprints** of this article or about obtaining **permission to reproduce this article** in whole or in part can be found at:

<http://www.sciencemag.org/about/permissions.dtl>

Regulation of Replication Fork Progression Through Histone Supply and Demand

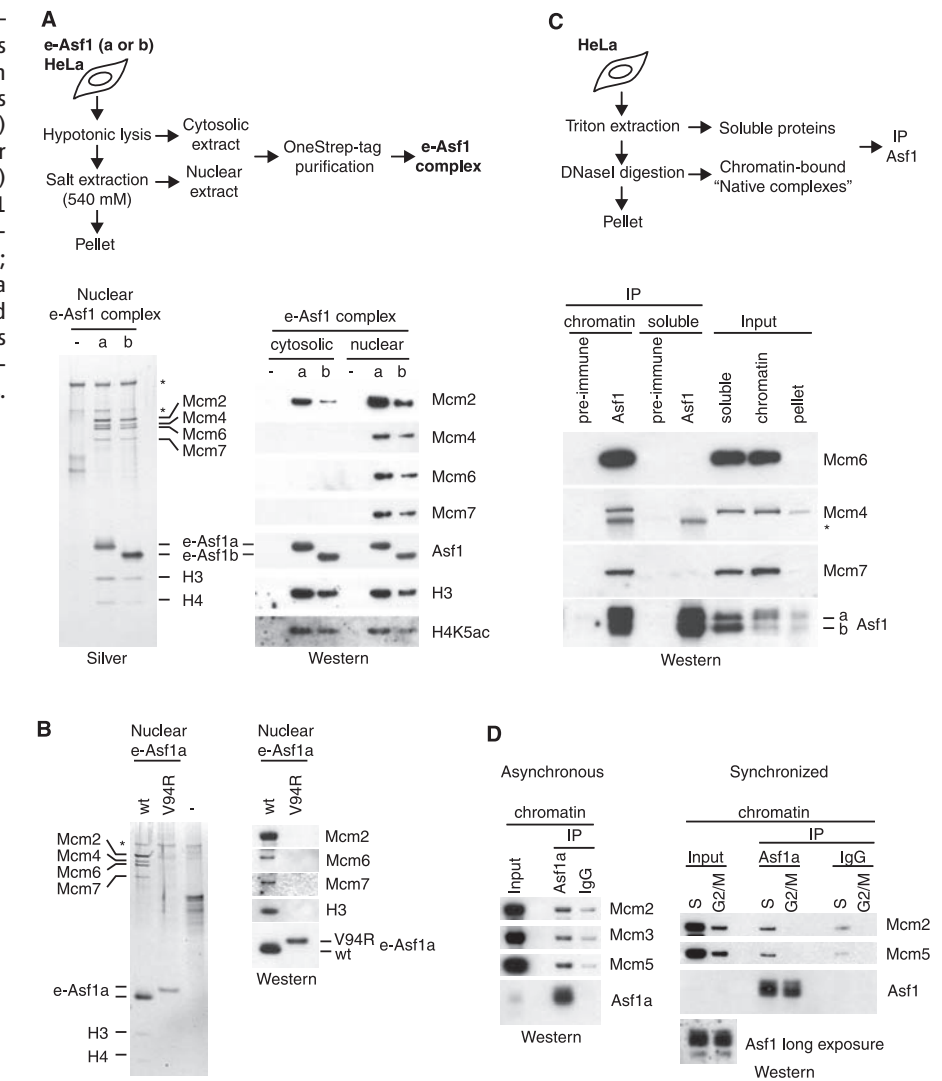
Anja Groth,¹ Armelle Corpet,¹ Adam J. L. Cook,¹ Daniele Roche,¹ Jiri Bartek,² Jiri Lukas,² Geneviève Almouzni^{1*}

DNA replication in eukaryotes requires nucleosome disruption ahead of the replication fork and reassembly behind. An unresolved issue concerns how histone dynamics are coordinated with fork progression to maintain chromosomal stability. Here, we characterize a complex in which the human histone chaperone Asf1 and MCM2–7, the putative replicative helicase, are connected through a histone H3–H4 bridge. Depletion of Asf1 by RNA interference impedes DNA unwinding at replication sites, and similar defects arise from overproduction of new histone H3–H4 that compromises Asf1 function. These data link Asf1 chaperone function, histone supply, and replicative unwinding of DNA in chromatin. We propose that Asf1, as a histone acceptor and donor, handles parental and new histones at the replication fork via an Asf1–(H3–H4)–MCM2–7 intermediate and thus provides a means to fine-tune replication fork progression and histone supply and demand.

When one parental nucleosome is disrupted ahead of the moving replication fork, two new nucleosomes, using new and recycled histones, must assemble on the

daughter strands to reproduce nucleosomal density (fig. S1A) (1). The regulatory link between histone biosynthesis and DNA replication (2) ensures the supply of new histones at the global level.

Fig. 1. Characterization of a human Asf1–(H3–H4)–MCM2–7 complex. **(A)** Purification scheme and analysis of e-Asf1 complexes by silver staining (left) and Western blotting (right). Control extract without e-Asf1 (–) was included to identify unspecific proteins (asterisks). **(B)** Silver staining and Western blot analysis of nuclear complexes containing wild-type (wt) or mutant (V94R) e-Asf1a. **(C)** Fractionation scheme and analysis of Asf1 immunoprecipitates (IP) from soluble and chromatin-bound material. The asterisk marks an unspecific band; input is 10% of starting material. **(D)** Analysis of Asf1a immunoprecipitates from asynchronous (left) and synchronized cells (right) (see also fig. S2D). Input is 3% of starting material. Under low-stringency conditions, some MCMs bind unspecifically to control beads.



However, an additional layer of regulation must be at play locally at individual replication forks to ensure balanced deposition of new and parental histones on the daughter strands. This may involve histone chaperones, such as Asf1 (antisilencing function 1), that can participate in both nucleosome assembly and disassembly (1, 3). Human Asf1a and Asf1b exist in two pools (4), a highly mobile (cytosolic) pool that buffers excess soluble histones during replication stress and a salt-extractable pool in nuclear extracts. How the latter relates to other chromatin proteins and contributes to nuclear function remains open.

We isolated and characterized *in vivo* complexes containing Asf1a or Asf1b, using stable HeLa S3 cell lines expressing tagged Asf1 (e-Asf1) (5). Mass spectrometry and Western blotting revealed the presence of Mcm2, 4, 6, and 7 in

¹Laboratory of Nuclear Dynamics and Genome Plasticity, UMR218 CNRS/Institut Curie, 26 rue d'Ulm, 75248 Paris cedex 05, France. ²Institute of Cancer Biology and Centre for Genotoxic Stress Research, Danish Cancer Society, Strandboulevarden 49, Copenhagen DK-2100, Denmark.

*To whom correspondence should be addressed. E-mail: Genevieve.Almouzni@curie.fr

the nuclear e-Asf1 (a and b) complexes, together with histone H3 and H4 (Fig. 1A and fig. S1B). By comparison, only Mcm2 was associated with cytosolic e-Asf1 (a and b) complexes. Antibodies against Mcm6 coimmunoprecipitated Asf1 and

histone H3-H4 from nuclear extracts (fig. S1C), whereas Mcm2, 4, and 7 were retrieved from both cytosolic and nuclear fractions. Given that this set of MCM proteins copurifies on histone H3-H4 columns (6), we tested whether Asf1 associates with

Mcm2, 4, 6, and 7 through histone H3-H4 by isolating complexes containing e-Asf1a mutated in the histone-binding domain, by replacement of valine at codon 94 with arginine (V94R) (7). e-Asf1a V94R did not bind histones H3-H4, as expected, and concomitantly MCMs were lost from the complex (Fig. 1B), which implicated histone H3-H4 in bridging the interaction between Asf1 and MCMs. To further confirm the chromatin link and to avoid the use of salt-extraction, which disrupts MCM2-7 hexamers into subcomplexes (6, 8) (fig. S1C), we used deoxyribonuclease (DNase I)-solubilized chromatin (Fig. 1C and fig. S2A). Again, Mcm2, 4, 6, and 7 coimmunoprecipitated with Asf1 (Fig. 1, C and D), and Mcm6 antibodies retrieved Asf1 (a and b) (fig. S2B). Under these conditions, which preserve the hexameric MCM2-7 complex (8) (fig. S2B), Mcm3 and Mcm5 coimmunoprecipitated with Asf1 (Fig. 1D), which was also confirmed by epitope tag purification of e-Asf1 complexes from chromatin (fig. S2C). This interaction on chromatin occurred in S phase (Fig. 1D), which suggested a role in DNA replication.

S-phase defects have been reported in various systems upon interference with Asf1 function (4, 9, 10). Human cells depleted of Asf1 (a and b) accumulated in S phase (Fig. 2A) with reduced 5-bromo-2'-deoxyuridine (BrdU) incorporation (fig. S3C). However, the appearance and distribution of replication factories marked by proliferating cell nuclear antigen (PCNA) and the pattern of chromatin-bound Mcm2 were unchanged (fig. S3), which was consistent with findings in *Drosophila* (10). Given the link with MCM2-7, considered to be the replicative helicase (11), we wondered whether inefficient replication could reflect problems of unwinding DNA in the context of chromatin. If so, the level of single-stranded DNA (ssDNA) at replication sites might be reduced. To monitor ssDNA at replication sites, we used two markers, replication protein A (RPA), which binds ssDNA, and PCNA, a polymerase accessory factor. In control cells, both RPA and PCNA showed characteristic replication patterns (Fig. 2A and fig. S4A). Although PCNA patterns were unchanged in Asf1-depleted cells, RPA replication patterns were barely detectable. Some nonextractable RPA localized to bright nuclear foci, which we identified as promyelocytic leukemia (PML) nuclear bodies, clearly distinct from PCNA replication foci (fig. S4B). We verified that Asf1 depletion did not affect RPA expression (fig. S3A) or its ability to bind ssDNA (fig. S5). Thus, absence of RPA replication profiles is consistent with the hypothesis of a helicase defect.

To examine helicase function, we analyzed DNA unwinding in the absence of polymerase progression by treating cells with hydroxyurea (HU) to deplete the nucleotide pool, which inhibits the DNA polymerase and leads to formation of ssDNA (12). In *Xenopus*, this response is dependent on MCM2-7 function (13). We measured formation of ssDNA ahead of the polymerase by detection of BrdU-substituted DNA and acute accumulation of RPA at replication sites (fig. S6). In control cells treated with HU, 75% of cells in S

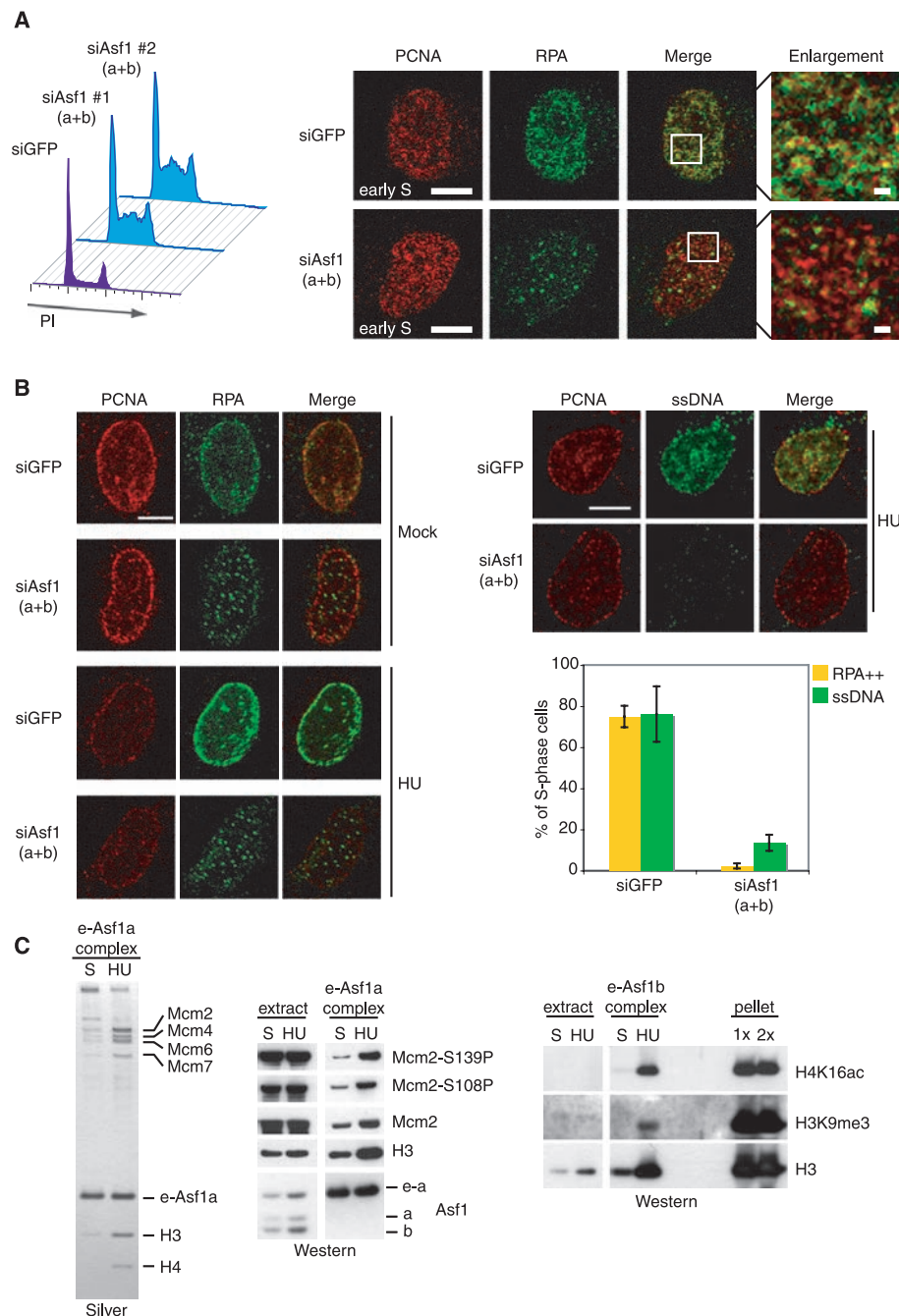


Fig. 2. Asf1 depletion impairs DNA unwinding. **(A)** (Left) Cell cycle profile of U-2-OS cells treated with small interfering RNAs (siRNAs) against Asf1a and Asf1b or control siRNA against GFP (siGFP). (Right) RPA and PCNA replication profiles in preextracted siRNA-treated cells. Images representative of five experiments show early S-phase cells with enlargements (4 \times). Cells in mid and late S phase showed similar defects (fig. S4A). Scale bars, 10 μ m and 1 μ m. **(B)** RPA accumulation (left) and ssDNA formation (right) after 1 hour of HU treatment (3 mM). For ssDNA analysis, BrdU was detected without double-stranded DNA (dsDNA) denaturation in cells prelabeled throughout their genome before HU treatment (fig. S6) (26). Scale bars, 10 μ m. (Lower right) Quantification of PCNA-positive cells with RPA accumulation (yellow) and ssDNA formation (green). Error bars indicate standard deviation in three experiments [$n > 400$ (RPA++), $n > 130$ (ssDNA)]. **(C)** Analysis of nuclear e-Asf1 complexes purified from S-phase cells treated with or without HU, in parallel with nucleosomal histones from pellet material (1 \times corresponds to same cell numbers as the nuclear extract).

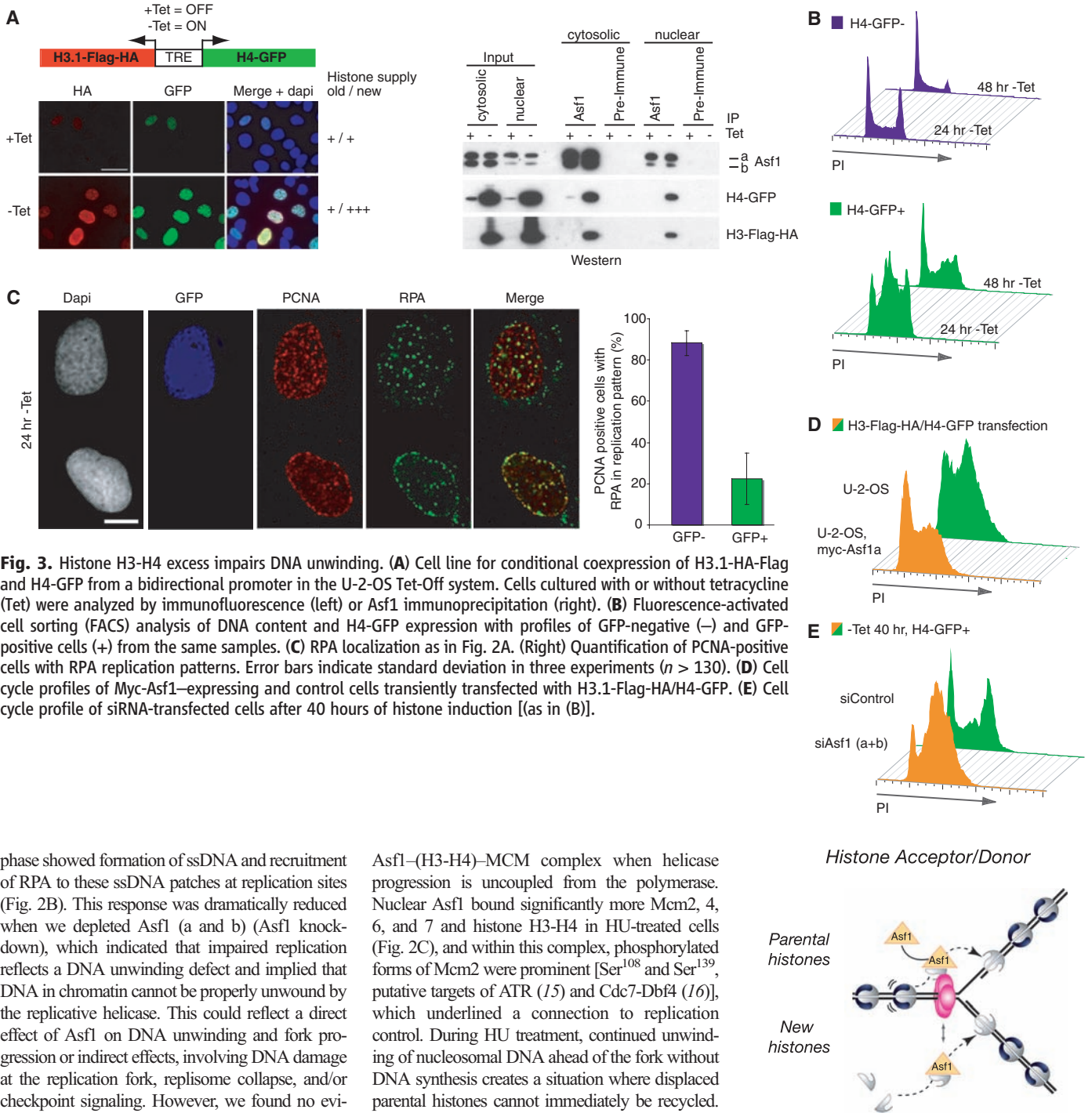


Fig. 3. Histone H3-H4 excess impairs DNA unwinding. **(A)** Cell line for conditional coexpression of H3.1-HA-Flag and H4-GFP from a bidirectional promoter in the U-2-OS Tet-Off system. Cells cultured with or without tetracycline (Tet) were analyzed by immunofluorescence (left) or Asf1 immunoprecipitation (right). **(B)** Fluorescence-activated cell sorting (FACS) analysis of DNA content and H4-GFP expression with profiles of GFP-negative (–) and GFP-positive cells (+) from the same samples. **(C)** RPA localization as in Fig. 2A. (Right) Quantification of PCNA-positive cells with RPA replication patterns. Error bars indicate standard deviation in three experiments ($n > 130$). **(D)** Cell cycle profiles of Myc-Asf1-expressing and control cells transiently transfected with H3.1-Flag-HA/H4-GFP. **(E)** Cell cycle profile of siRNA-transfected cells after 40 hours of histone induction [(as in B)].

phase showed formation of ssDNA and recruitment of RPA to these ssDNA patches at replication sites (Fig. 2B). This response was dramatically reduced when we depleted Asf1 (a and b) (Asf1 knock-down), which indicated that impaired replication reflects a DNA unwinding defect and implied that DNA in chromatin cannot be properly unwound by the replicative helicase. This could reflect a direct effect of Asf1 on DNA unwinding and fork progression or indirect effects, involving DNA damage at the replication fork, replisome collapse, and/or checkpoint signaling. However, we found no evidence of DNA damage or checkpoint activation upon Asf1 knockdown (fig. S7A), and consistently, checkpoint abrogation by caffeine did not rescue the unwinding defect (fig. S7B). Instead, induction of γ -H2AX (phosphorylation of a histone 2A variant) in response to HU treatment was impaired in Asf1-depleted cells (fig. S7D), which was consistent with a role of ssDNA in checkpoint signaling (12, 14). Furthermore, expression and chromatin association of several key replication factors remained unchanged upon Asf1 knockdown (fig. S7C).

To explore whether a direct role of Asf1 in facilitating DNA unwinding could involve interaction with histones and MCM2–7, we followed the

Asf1–(H3-H4)–MCM complex when helicase progression is uncoupled from the polymerase. Nuclear Asf1 bound significantly more Mcm2, 4, 6, and 7 and histone H3-H4 in HU-treated cells (Fig. 2C), and within this complex, phosphorylated forms of Mcm2 were prominent [Ser¹⁰⁸ and Ser¹³⁹, putative targets of ATR (15) and Cdc7-Dbf4 (16)], which underlined a connection to replication control. During HU treatment, continued unwinding of nucleosomal DNA ahead of the fork without DNA synthesis creates a situation where displaced parental histones cannot immediately be recycled. The accumulation of Asf1–(H3-H4)–MCM complexes under such conditions suggests that this complex could be an intermediate in parental histone transfer. Within these complexes, we could detect histone modifications, H4 with acetylated lysine 16 (H4K16Ac) and H3 with trimethylated lysine 9 (H3K9me3) (Fig. 2C). This further substantiates our hypothesis, as these chromatin marks are poorly represented on newly synthesized histones (17–19).

Our results suggest that Asf1 coordinates histone supply (parental and new) with replication fork progression. To manipulate new histone supply, we generated a conditional cell line for coexpression of

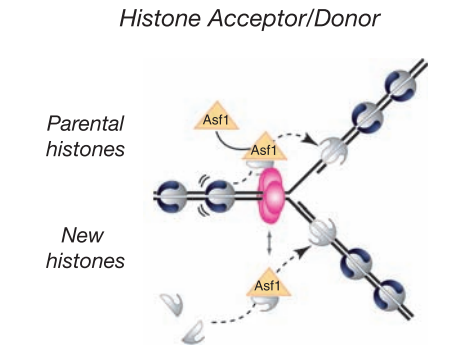


Fig. 4. Model for Asf1 function in replication as a histone acceptor and donor.

tagged histone H3.1 and H4 (Fig. 3A). About 50% of the cells expressed H3.1-H4 when tetracycline was removed, and Asf1 bound the exogenous histones (Fig. 3A). After induction, the nonnucleosomal histone pool increased two- to threefold (fig. S8A), a range that is comparable to histone overload during a replication block (4). Increasing new histone supply interfered with DNA replication and caused acute accumulation of H3.1-H4 over-expressing cells in S phase [tracked by the green

fluorescent protein (GFP) tag on H4] (Fig. 3B). At later time points, the majority of GFP-positive cells arrested in late S/G₂. We focused on the S-phase defect to address whether H3-H4 excess mimicked Asf1 depletion. The moderate increase in H3-H4 expression did not cause DNA damage monitored by γ -H2AX (fig. S8B). We thus analyzed RPA and PCNA profiles using GFP-negative cells (no H3.1-H4 induction) as an internal control for proper localization (Fig. 3C). Again, as in Asf1-depleted cells, RPA replication patterns in histone-over-expressing cells were barely visible, with some RPA localized to bright nuclear foci mainly corresponding to PML bodies (Fig. 3C and fig. S8D). Furthermore, as for Asf1 knockdown, an excess of new H3-H4 histones impaired ssDNA formation and RPA accumulation at replication sites (fig. S9, A and B), as well as checkpoint activation in response to HU (figs. S9C and S8C). Together, these data indicate that overproduction of histone H3-H4 impairs replication by impeding DNA unwinding. Consistent with the possibility that this results from interference with Asf1 function, we found that ectopic expression of Asf1a partially alleviated the inhibitory effect of histone excess on S-phase progression (Fig. 3D). Moreover, Asf1 depletion aggravated the S-phase defect resulting from histone H3-H4 excess, in that progression into G₂ was delayed even further (Fig. 3E).

Together, our results show that replication fork progression is dependent on the histone H3-H4 chaperone, Asf1, and on an equilibrium between histone supply and demand. This dependency could ensure that replication only proceeds when nucleosomes are being formed behind the fork with a proper balance between new and parental histones H3-H4. In the most parsimonious view, we propose a model (Fig. 4) in which Asf1 uses its properties as a histone acceptor and donor to facilitate unwinding

of the parental chromatin template in coordination with nucleosome assembly on daughter strands. Nucleosome disruption during replication fork passage would involve the histone-binding capacity of the MCM2–7 complex and transfer of parental histones to Asf1 through the Asf1–(H3-H4)–MCM intermediate, followed by their deposition onto daughter strands. In parallel, Asf1 would provide the additional complement of histones through its established role as a new histone donor (4, 20, 21). Asf1 knockdown will impair histone transfer and disruption of parental nucleosomes that thus present an impediment to unwinding and replication fork progression. Similarly, because of the dual function of Asf1, an excess of new histones will not leave Asf1 available for parental transfer, which impairs unwinding. On the basis of structural data (7, 22, 23), our model implies that parental histones (H3-H4)₂, like new histones (24), go through a transient dimeric state during transfer. Furthermore, the MCM–(H3-H4)–Asf1 connection opens new angles to understand MCM2–7 function in chromatin (25). In conclusion, having Asf1 deal with both new and parental histones could provide an ideal means to fine-tune de novo deposition and recycling with replication fork progression. By offering a mechanism to coordinate new and parental histones during replication, our model should pave the way to addressing key questions regarding chromatin-based inheritance, including transmission of histone modifications.

References and Notes

1. A. Groth, W. Rocha, A. Verreault, G. Almouzni, *Cell* **128**, 721 (2007).
2. A. Gunjan, J. Paik, A. Verreault, *Biochimie* **87**, 625 (2005).
3. B. Li, M. Carey, J. L. Workman, *Cell* **128**, 707 (2007).
4. A. Groth *et al.*, *Mol. Cell* **17**, 301 (2005).
5. Materials and methods are available as supporting material on *Science* Online.

6. Y. Ishimi, S. Ichinose, A. Omori, K. Sato, H. Kimura, *J. Biol. Chem.* **271**, 24115 (1996).
7. F. Mousson *et al.*, *Proc. Natl. Acad. Sci. U.S.A.* **102**, 5975 (2005).
8. M. Fujita, T. Kiyono, Y. Hayashi, M. Ishibashi, *J. Biol. Chem.* **272**, 10928 (1997).
9. F. Sanematsu *et al.*, *J. Biol. Chem.* **281**, 13817 (2006).
10. L. L. Schulz, J. K. Tyler, *FASEB J.* **20**, 488 (2006).
11. T. S. Takahashi, D. B. Wigley, J. C. Walter, *Trends Biochem. Sci.* **30**, 437 (2005).
12. D. Shechter, V. Costanzo, J. Gautier, *DNA Repair (Amsterdam)* **3**, 901 (2004).
13. M. Patek, J. C. Walter, *EMBO J.* **23**, 3667 (2004).
14. T. S. Byun, M. Patek, M. C. Yee, J. C. Walter, K. A. Cimprich, *Genes Dev.* **19**, 1040 (2005).
15. D. Cortez, G. Glick, S. J. Elledge, *Proc. Natl. Acad. Sci. U.S.A.* **101**, 10078 (2004).
16. T. Tsuji, S. B. Ficarro, W. Jiang, *Mol. Biol. Cell* **17**, 4459 (2006).
17. L. J. Benson *et al.*, *J. Biol. Chem.* **281**, 9287 (2006).
18. A. Loyola, T. Bonaldi, D. Roche, A. Imhof, G. Almouzni, *Mol. Cell* **24**, 309 (2006).
19. R. E. Sobel, R. G. Cook, C. A. Perry, A. T. Annunziato, C. D. Allis, *Proc. Natl. Acad. Sci. U.S.A.* **92**, 1237 (1995).
20. J. A. Mello *et al.*, *EMBO Rep.* **3**, 329 (2002).
21. J. K. Tyler *et al.*, *Nature* **402**, 555 (1999).
22. C. M. English, M. W. Adkins, J. J. Carson, M. E. Churchill, J. K. Tyler, *Cell* **127**, 495 (2006).
23. R. Natsume *et al.*, *Nature* **446**, 338 (2007).
24. H. Tagami, D. Ray-Gallet, G. Almouzni, Y. Nakatani, *Cell* **116**, 51 (2004).
25. R. A. Laskey, M. A. Madine, *EMBO Rep.* **4**, 26 (2003).
26. E. Raderschall, E. I. Golub, T. Haaf, *Proc. Natl. Acad. Sci. U.S.A.* **96**, 1921 (1999).
27. We thank P. Le Baccon, W. Faigle, E. Heard, A. Loyola, and A. Probst. Supported by Canceropole, Danish Cancer Society, Danish Research Council, Danish National Research Foundation, Ligue Nationale contre le Cancer, MSM6198959216, NoE Epigenome, and University of Paris 6.

Supporting Online Material

www.sciencemag.org/cgi/content/full/318/5858/1928/DC1
Materials and Methods
Figs. S1 to S9
References

9 August 2007; accepted 1 November 2007
10.1126/science.1148992

Switching from Repression to Activation: MicroRNAs Can Up-Regulate Translation

Shobha Vasudevan, Yingchun Tong, Joan A. Steitz*

AU-rich elements (AREs) and microRNA target sites are conserved sequences in messenger RNA (mRNA) 3' untranslated regions (3'UTRs) that control gene expression posttranscriptionally. Upon cell cycle arrest, the ARE in tumor necrosis factor- α (TNF α) mRNA is transformed into a translation activation signal, recruiting Argonaute (AGO) and fragile X mental retardation-related protein 1 (FXR1), factors associated with micro-ribonucleoproteins (microRNPs). We show that human microRNA miR369-3 directs association of these proteins with the AREs to activate translation. Furthermore, we document that two well-studied microRNAs—Let-7 and the synthetic microRNA miRxcxr4—likewise induce translation up-regulation of target mRNAs on cell cycle arrest, yet they repress translation in proliferating cells. Thus, activation is a common function of microRNPs on cell cycle arrest. We propose that translation regulation by microRNPs oscillates between repression and activation during the cell cycle.

AU-rich elements (AREs) bind specific proteins to regulate mRNA stability or translation in response to external and internal stimuli (1). MicroRNAs are small non-

coding RNAs that recruit an Argonaute (AGO) protein complex to a complementary target mRNA, which results in translation repression or degradation of the mRNA (2, 3). We previously dem-

onstrated that the tumor necrosis factor- α (TNF α) ARE can be transformed by serum starvation, which arrests the cell cycle, into a translation activation signal (4). AGO2 and fragile X mental retardation-related protein 1 (FXR1) associate with the ARE on translation activation; both proteins are required to increase translation efficiency. Two key questions arose. First, is binding of the AGO2-FXR1 complex, which activates translation, directed by a microRNA complementary to the ARE? Second, can micro-ribonucleoproteins (microRNPs), in general, up-regulate translation under growth-arrest conditions, thereby switching between repressing and activating roles in response to the cell cycle?

A bioinformatic screen identified five microRNAs in miRBASE with seed regions complementary to the TNF α ARE, not including miR16 (5) [see supporting online material (SOM) text]. Of these, only human miR369-3 (Fig. 1A and fig. S1) tested positive in the following assays. Its seed sequence potentially forms base pairs with two target sites [seed1 and seed2, shaded in (Fig. 1A)] within the minimal TNF α ARE needed for translation activa-